Novel insights into old anticancer drugs

Zanden, S.Y. van der

Citation

Zanden, S. Y. van der. (2021, March 2). *Novel insights into old anticancer drugs*. Retrieved from https://hdl.handle.net/1887/3135058

Cover Page

Universiteit Leiden

Author: Zanden, S.Y. van der
Title: Novel insights into old anticancer drugs
Issue date: 2021-03-02
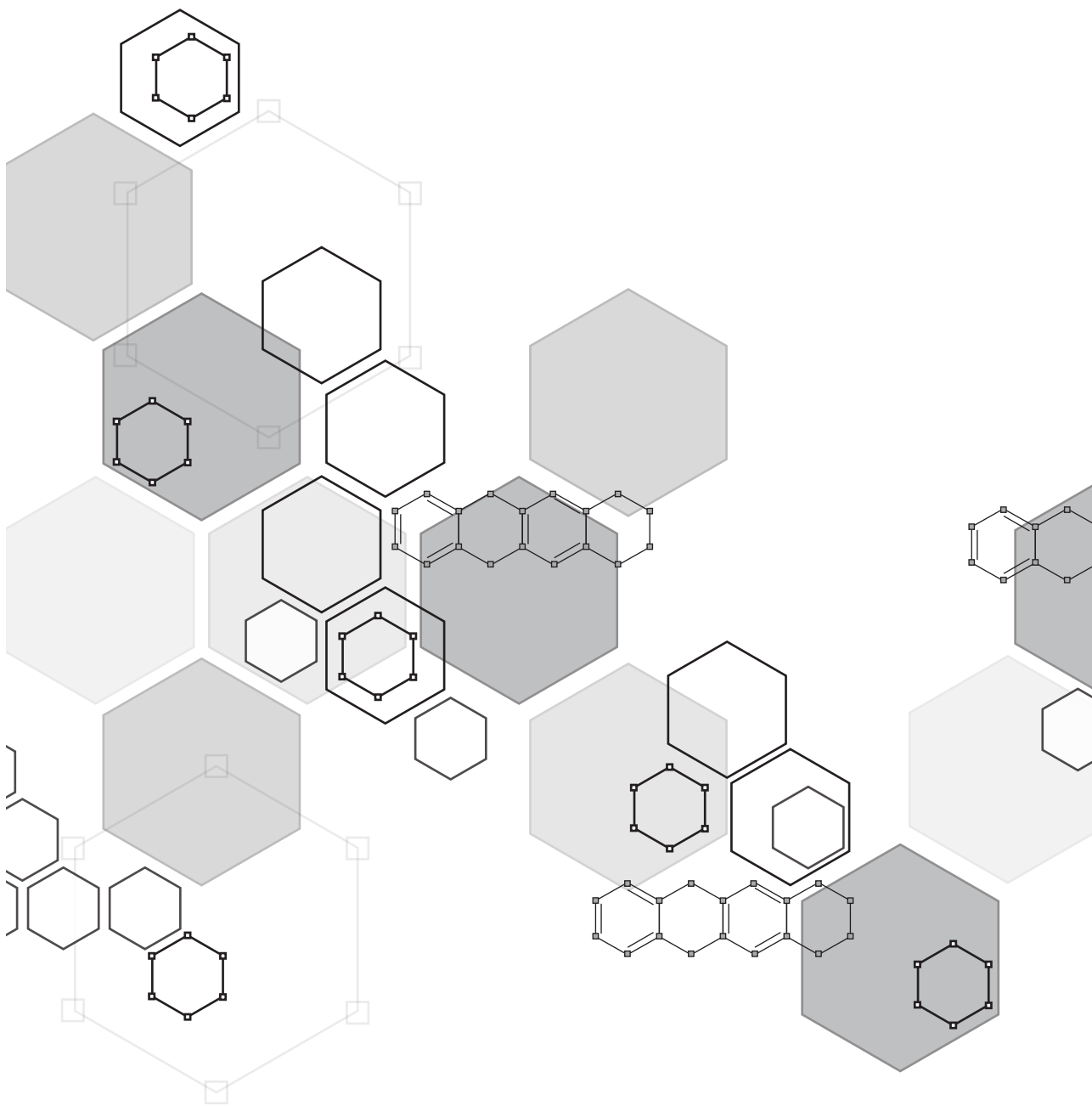
Genome-wide identification and characterization of novel factors conferring resistance to topoisomerase II poisons in cancer

2

Ruud H. Wijdeven#, Baoxu Pang#, Sabina Y. van der Zanden, Xiaohang Qiao, Vincent Blomen, Marlous Hoogstraat, Esther H. Lips, Lennert Janssen, Lodewyk Wessels, Thijn R. Brummelkamp and Jacques Neefjes

#These authors contributed equally

ABSTRACT

The Topoisomerase II poisons doxorubicin and etoposide constitute longstanding cornerstones of chemotherapy. Despite their extensive clinical use, many patients do not respond to these drugs. Using a genome-wide gene knockout approach, we identified Keap1, the SWI/SNF complex, and C9orf82 as independent factors capable of driving drug resistance through diverse molecular mechanisms, all converging on the DNA double-strand break (DSB) and repair pathway. Loss of Keap1 or the SWI/SNF complex inhibits generation of DSB by attenuating expression and activity of topoisomerase IIα, respectively, while deletion of C9orf82 augments subsequent DSB repair. Their corresponding genes, frequently mutated or deleted in human tumors, may impact drug sensitivity, as exemplified by triple-negative breast cancer patients with diminished SWI/SNF core member expression who exhibit reduced responsiveness to chemotherapy regimens containing doxorubicin. Collectively, our work identifies genes that may predict the response of cancer patients to the broadly used topoisomerase II poisons and defines alternative pathways that could be therapeutically exploited in treatment-resistant patients.

INTRODUCTION

Topoisomerase II (Topo II) poisons, including those of the anthracycline and podophyllotoxin families, are among the major classes of chemotherapeutics used to treat a wide spectrum of tumors. These drugs trap Topo II onto the DNA and inhibit DNA re-ligation, hereby 'poisoning' the enzyme and generating DNA double-strand breaks [1]. Despite their broad applicability, resistance constitutes a frequent clinical limitation [2]. Given the serious side effects associated with their administration, development of a comprehensive panel of treatment predicting factors could provide a useful clinical tool for matching chemotherapy to individual patients [1].

Anthracyclines, with doxorubicin (Doxo) as their prominent example, constitute an especially effective class of anti-cancer drugs, as they intercalate into the DNA and evict histones from the chromatin, concomitant to inhibiting Topo II after the formation of a DNA double-strand break [3, 4]. As a result, the DNA damage response is attenuated and the epigenome becomes deregulated at defined regions in the genome [3, 5]. The cellular pathways contributing to Doxo resistance have been interrogated extensively, and the drug transporter ABCB1 (MDR1), capable of exporting Doxo from cells [2], has emerged as a major player in this context. Despite its role in drug removal at the blood-brain barrier, inhibition of ABCB1 failed to satisfactorily revert unresponsiveness to Doxo in the clinic [6]. Other factors, acting either alone or in combination with proteins such as ABCB1, have been implicated in Doxo resistance through the downregulation of either Topo II or other DNA damage response (DDR) pathway constituents [7, 8]. Thus far, none of the above factors have been shown to individually account for the observed variability in patients' responses to Doxo [1, 9]. Taken together, the findings reported to date suggest the existence of other as of yet undefined molecular determinants instrumental in the conversion to a Doxo-resistant state.

Herein we report on a genome-wide screen for factors driving resistance to Doxo using a knockout approach in haploid cells [10]. With the aim of approximating the physiological situation of patient drug exposure—and by extension drug resistance—in the tissue culture environment, we iteratively subjected cells to Doxo for three brief periods as a means of selecting for relative drug resistance. Our screening methodology yielded two previously described contributors to drug resistance: the afore-

mentioned transporter ABCB1 [2] and the stress response gene Keap1 [11]. We also identified several novel factors: the gene product of C9orf82 that appears to function as an inhibitor of DNA damage repair and the chromatin remodeling SWI/SNF complex subunits SMARCB1 and SMARCE1. Depletion of either Keap1, C9orf82 or SMARCB1 was found to induce cellular resistance to Topo II poisons, without significantly affecting sensitivity to either Topo I inhibitors or aclarubicin (Acla), an analog of Doxo that does not induce DNA damage [3, 5]. All genes identified in the resistance screen were found to regulate Topo II-induced DNA break formation or subsequent DNA repair. In the clinic, tumors frequently harbor mutations or deletions in Keap1, C9orf82 or components of the SWI/SNF complex [12-14]. These may be relevant for patient stratification to Doxo-based therapies, as illustrated by the correlation between expression levels of Keap1 and the SWI/SNF complex subunits and the response of triple negative breast cancer patients to Doxo-based treatment. Our data provide a molecular basis for patient selection in the clinic with regards to the broadly used Topo II poisons in cancer therapy.

RESULTS
Identification and validation of doxorubicin-resistance factors Keap1, C9orf82 and the SWI/SNF complex

To identify genetic determinants involved in resistance to Doxo, we performed a genome-wide insertional mutagenesis screen in haploid cells using a gene trap retrovirus [10]. A genomic insertion of the virus into the sense direction of a gene disrupts its expression and often results in a complete knockout of the gene. HAP1 cells were infected with a gene trap retrovirus to generate a pool of randomly mutagenized cells and briefly passaged prior to drug exposure. To recapitulate the normal pharmacokinetics of Doxo in a tissue culture setting, we exposed these cells for 2 hours to 1μM Doxo, which is within the peak plasma dose of standard treatment of cancer patients [15]. Cells were treated weekly for three weeks, after which surviving cells were grown out and insertions were mapped and aligned to the human genome (Figure 1A). Disruptions of six genes were significantly enriched (p<0.00005) in the surviving population compared to the untreated control (Figure 1B and Table S1) Among these were two previously reported factors, ABCB1 [6] and Keap1 [16], as well as novel factors, including the SWI/SNF subunits, SMARCB1 and SMARCE1, the C9orf82 gene, and the translation initiation factor Eif4a1. Canonical Doxo-target Topo IIα appeared just below the threshold, with an adjusted p-value of 0.01. ABCB1 contained mostly anti-sense mutations following selection, which could enhance its expression (unpublished observation). All other enriched genes contained at least five independent insertions in the sense direction, leading to their inactivation. Identification of Keap1 provided validation of the screening methodology, as it has already been associated with resistance to several anti-cancer drugs, including Doxo [11, 12, 17]. To validate the screen hits, we generated HAP1 cells stably expressing either control shRNA or two independent shRNAs targeting Keap1, which reduced Keap1 expression by 50-80% (Figure 1C and S1A). These knockdown cell lines were subsequently exposed to Doxo for two hours, followed by drug wash out and outgrowth. As expected, Keap1 depletion conferred Doxo resistance as illustrated in both colony formation and viability assays (Figure 1D and S1B).

We then proceeded to validate the novel screen hits. Two independent CRISPR/Cas9 constructs targeting the SMARCB1 gene (Figure 1E) rendered the cells more resistant to Doxo, both in colony formation and viability assays (Figure 1F and S1C).
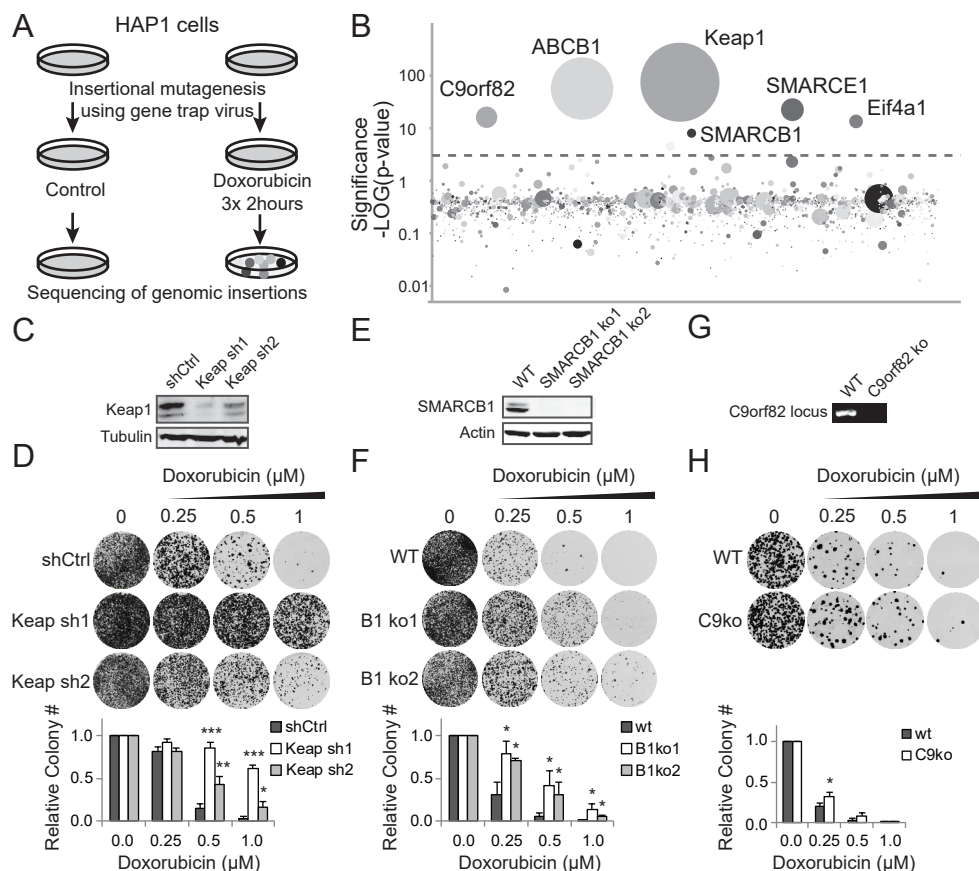
Figure 1. Genome-wide mutagenesis screen identifies Keap1, the SWI/SNF complex and C9orf82 as regulators of doxorubicin resistance. *(A) Schematic set-up of the haploid genetics screen to identify genes involved in Doxo resistance. (B) Screening results. The y axis indicates the significance of enrichment of gene-trap insertions in Doxo-treated compared to non-treated control cells. The circles represent genes and their size corresponds to the number of independent insertions mapped in the gene. For more hits, see Table S1. (C) Keap1 silencing was determined by Western blotting analysis. (D) Long-term colony formation assay with HAP1 cells transduced with shRNAs targeting Keap1 or a control shRNA. Cells were treated with the indicated concentration Doxo for 2h and left to grow out. After 9 days, cells were fixed, stained and imaged. Quantification of colony numbers per plate and condition from three independent experiments (± SD) are shown below the images. (E) Western blotting showing depletion of SmarcB1 by two independent CRISPR-targeting sequences. (F) Long term colony formation assays for wild-type and SMARCB1-depleted cells. Results from three independent experiments (± SD) were quantified and are shown below the images. (G) Genomic PCR showing the knockout of C9orf82. (H) Long-term colony formation assay for wild-type and C9orf82-depleted cells. Results from three independent experiments (± SD) were quantified and are shown below the images. Statistical significance was calculated compared to control (* p < 0.05, ** p < 0.01, *** p < 0.001).*

Independent identification of two members of the SWI/SNF chromatin-remodeling complex [18], SMARCB1 and SMARCE1, suggested that deregulation of the complex as a whole may drive resistance to Doxo. Although we could not validate a role

for SMARCE1 in resistance to Doxo, shRNA-mediated depletion of the SWI/SNF core members SMARCA4 and ARID1A, alongside SMARCB1, induced resistance to Doxo (Figure S1D and S1E), supporting the notion that loss of the SWI/SNF complex functionality confers resistance to Doxo.

While we did not further pursue the translational elongation complex subunit Eif4a1, we tested the contribution of the open reading frame 82 on chromosome 9 (C9orf82) to Doxo sensitivity. A small but significant growth advantage was observed in response to Doxo treatment in C9orf82 knockout cells using a colony formation assay (Figure 1G and 1H). Collectively, our genome-wide screen identified multiple novel factors capable of incurring resistance to Doxo in a cell culture setting.

Cross-resistance to other DNA-damaging drugs

Doxo is known to act on cells by a combination of Topo II poisoning, eviction of histones from the chromatin and the generation of reactive oxygen species (ROS) [3, 4, 19]. To establish which of these mechanisms are affected by Keap1, the SWI/SNF complex and C9orf82, we treated the respective knockdown or knockout cell lines with either the different Topo II poisons daunorubicin (Daun; an anthracycline with a structure and activity similar to Doxo) or etoposide (Etop; a Topo II poison structurally unrelated to Doxo and incapable of evicting histones), or with aclarubicin (Acla; an anthracycline family member that evicts histones, induces ROS and inhibits Topo II but does not induce DNA damage [20]). Silencing Keap1 or eliminating SMARCB1 or C9orf82 rendered cells more resistant to both Etop and Daun, but not Acla (Figure 2A-2C) as indicated by viability as well as colony formation assays. Given the properties of the three drugs, these observations provide hints as to the molecular mechanisms underlying Doxo resistance via these genes – through the DNA damage arm. Interestingly, C9orf82 depletion rendered cells more resistant to Etop than to Doxo or Daun, suggesting that fast DNA repair may be critical for this gene's mode of action, as Doxo and Daun attenuate DNA repair by eviction of H2AX [5].

Importantly, depletion of none of our hits induced measurable resistance to the topoisomerase I poison topotecan (TPT) that induces single-strand DNA breaks (Figure 2C and 2D), suggesting that Keap1, the SWI/SNF complex and C9orf82 are involved in the Topo II-dependent DDR pathway.

Keap1 controls the expression of Topo IIα independently of Nrf2

Of the three validated resistance factors from the screen, Keap1 has been previously linked to chemoresistance [11, 16, 21]. Keap1 functions as an E3 ligase adaptor and is known to mediate the degradation of Nrf2, a transcription factor for oxidative stress response genes [22]. Upregulation of Nrf2 desensitizes cells to several anti-cancer drugs, including alkylating and anti-mitotic agents, which suggests that downregulation of Keap1 may induce drug resistance by stabilizing Nrf2 [12, 16, 17]. To test this, we used CRISPR/Cas9 technology to generate Nrf2 knockout cells (Figure 3A), functionally validated by a drastic reduction of expression of Nrf2 target gene NQO1 (Figure S2A). Unexpectedly, silencing of Keap1 in the Nrf2 null background still endowed cells more resistance to Doxo and Etop (Figure 3A), implying the existence of an Nrf2-independent mechanism for Keap1 in modulating cellular responsiveness to Topo II dependent DNA-damage inducers.

Double-strand DNA break analysis indicated that loss of Keap1 significantly decreases the amount of such breaks induced by either Etop or Doxo treatment (Figure 3B). These results were corroborated by the observed reduction in the DNA damage response as measured by γ-H2AX following exposure to Etop (Doxo evicts H2AX
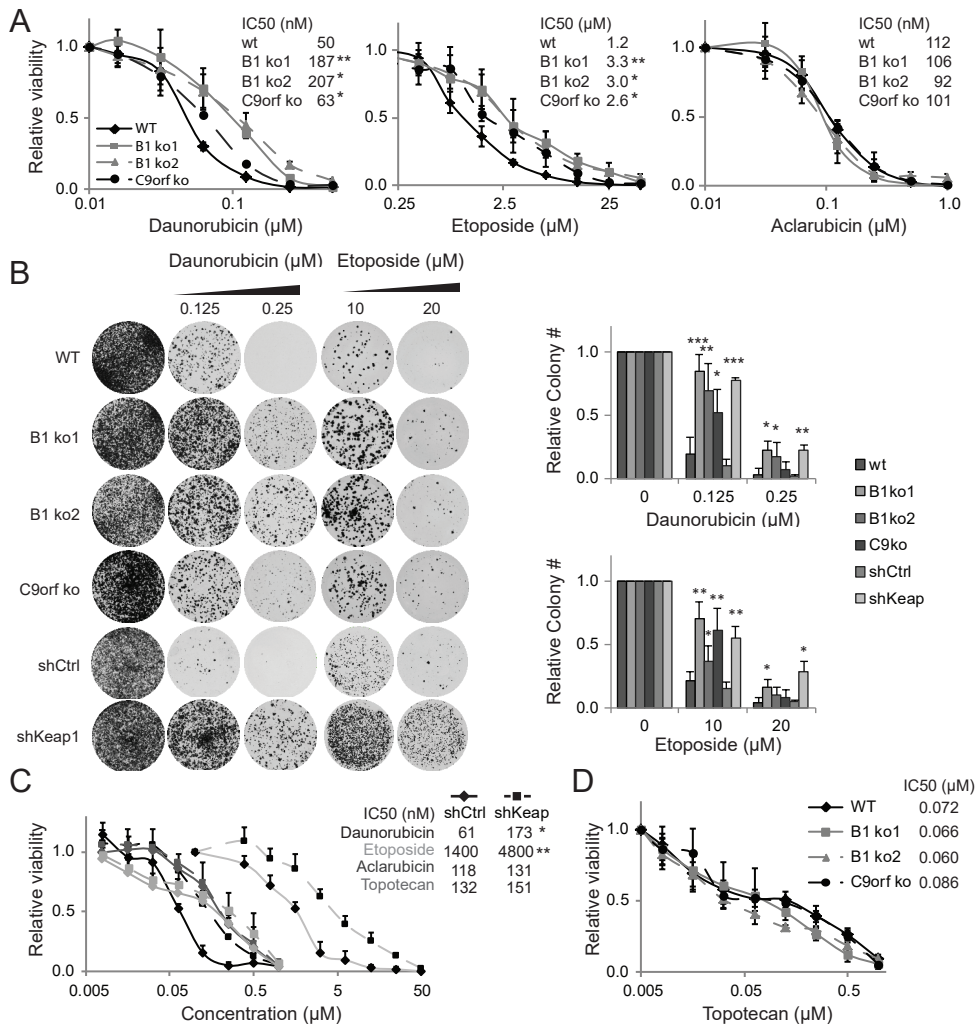
Figure 2. Keap1, SWI/SNF and C9orf82 control to sensitivity to TopoII but not the TopoI inhibitor or Acla. *(A) HAP1 cells depleted for SMARCB1 or C9orf82 were treated for 2h with Daun, Etop or Acla and cell viability was analyzed 72h later by a cell titer blue (CTB) assay. (B) Long term colony formation assay with HAP1 cells depleted for SMARCB1, C9orf82 or Keap1 that were treated for 2h with the indicated drug at different concentrations. (C) HAP1 cells stably expressing shCtrl or shKeap1 were treated for 2h with Daun, Etop, Acla or topotecan and cell viability was analyzed 72h later by a CTB assay. (D) HAP1 cells depleted for SMARCB1 or C9orf82 were treated for 2h with TPT and cell viability was analyzed 72h later by a CTB assay. All experiments shown are representatives of at least three independent experiments. Statistical significance was calculated as compared to control cells (* p < 0.05, ** p < 0.01, *** p < 0.001).*

from the DNA and was therefore not used to measure the DDR after drug exposure) (Figure 3C). Keap1 silencing did not affect uptake of Doxo (monitored by intrinsic fluorescence of the drug by flow cytometry, Figure 3D), suggesting that Keap1 may control either the levels or activity of the drug target, Topo IIα. Cells depleted of
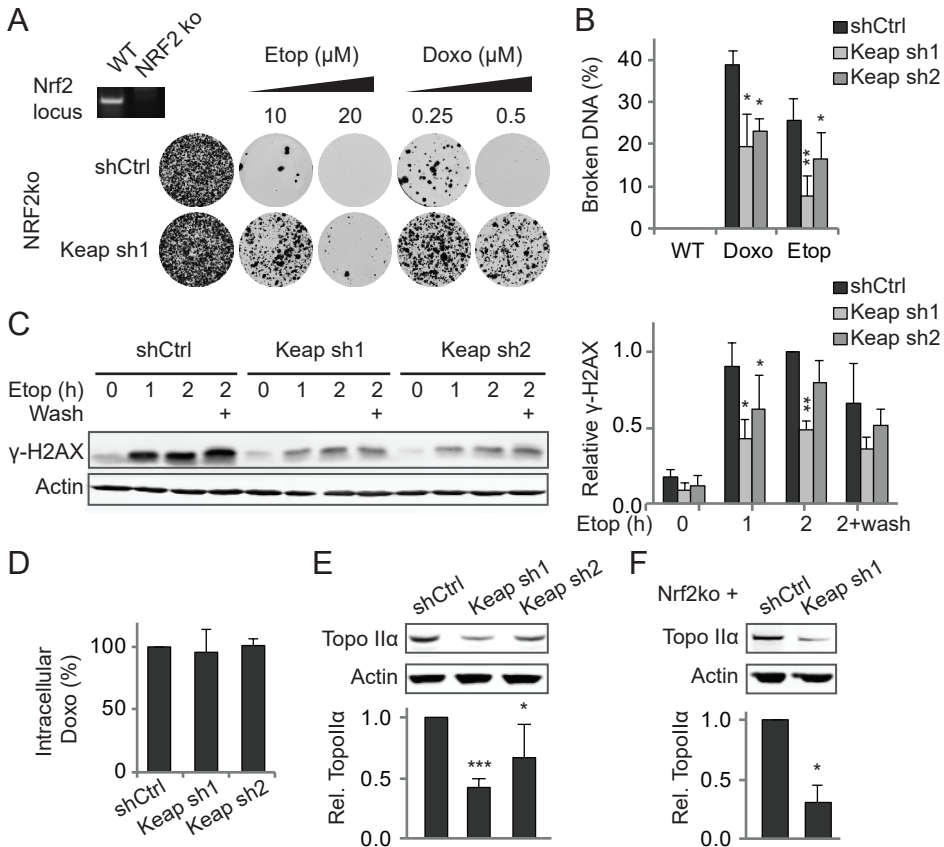
Figure 3. Keap1 controls Topo IIα expression independently of Nrf2. *(A) Long-term colony growth assay for HAP1 cells depleted for Nrf2 and further stably transduced with shKeap1 or shCtrl. Cells were treated for 2h with Doxo or Etop at the indicated concentrations and left to grow out for 9 days. Insert: the DNA gel shows loss of the genomic Nrf2 locus in the knockout cells. (B) Analysis of the amount of Etop- or Doxo-induced DNA breaks using constant field gel electrophoresis. HAP1 cells were treated for 2h with 1µM Etop or Doxo, lysed and analyzed. Shown is the quantification of the broken DNA relative to input. (C) HAP1 cells were treated with 5µM Etop for the indicated time points, or the drug was washed out after 2h and cells were left to recover for another 2h (lanes '+'), lysed and analyzed by SDS-PAGE and Western blotting. Right: quantification of the γ-H2AX signal normalized to actin. The signal of wild-type cells treated for 2h was set at 1. (D) Cells were treated with 2µM Doxo for 1h and Doxo levels were analyzed using flow cytometry. Control shRNA was set at 1. (E) Western blotting analysis for expression of Topo IIα in HAP1 cells silenced for Keap1. For quantification, the signal is normalized to actin and the shCtrl was set at 1. (F) Western blotting analysis for expression of Topo IIα in HAP1 Nrf2ko cells stably depleted or not for Keap1. All results are mean ± SD of biological triplicates, except for (E), which are biological quadruplicates. Statistical significance was calculated compared to control (* p < 0.05, ** p < 0.01, *** p < 0.001).*

Keap1 had lower Topo IIα expression levels relative to the control (Figure 3E), which was independent of Nrf2 activity (Figure 3F). A link between Topo IIα expression levels and resistance against Topo II poisons has been previously suggested [7, 23, 24]. These observations indicate that Keap1 can control resistance to Topo II poisons by two distinct mechanisms—regulating Nrf2 expression to control a series

of stress-response genes and by mediating the expression of the canonical target Topo IIα.

C9orf82 regulates repair of DNA damage induced by TopoII poisons

By contrast to the previously studied role of Keap1 in drug resistance, the role of C9orf82 in this context has not been addressed, with its only function thus far assigned being negative regulation of apoptosis [25]. We began by addressing the effect of this gene on Topo II induced DSB formation and repair as pertaining to Topo II function. Monitoring the DNA DSBs and the resulting DNA damage response following exposure to either Doxo or Etop revealed no difference in the initial levels of DNA damage incurred between the control and C9orf82 knockout cells (Figure 4A and 4B). Strikingly, the resolution of the DNA damage response signal following Etop treatment (as visualized by γ-H2AX) was significantly accelerated in C9orf82 knockout cells (Figure 4B). Similar results were obtained with another independently
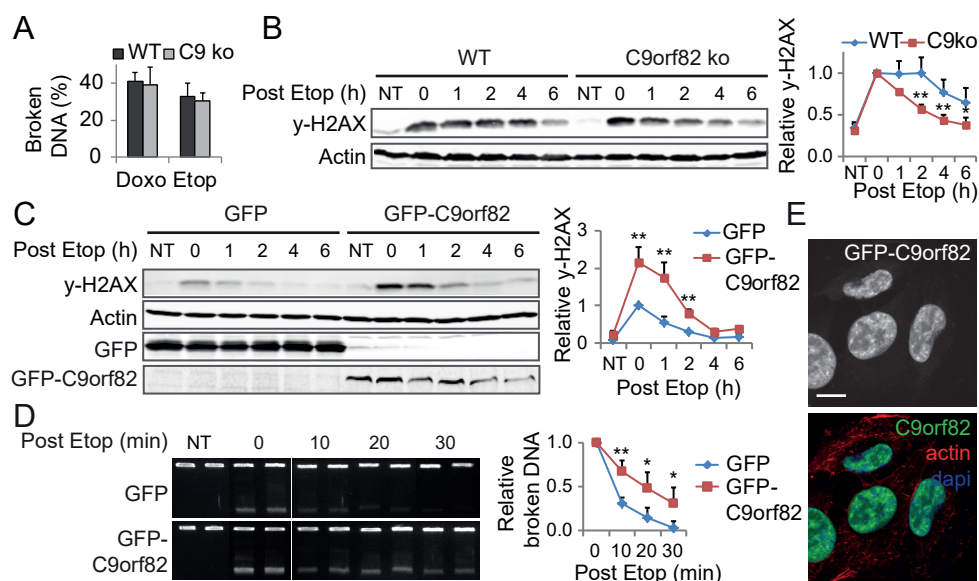

Figure 4. C9orf82 regulates DNA double-strand break repair. *(A) Analysis of the amount of Etop- or Doxo-induced DNA breaks using constant field gel electrophoresis. HAP1 cells were treated for 2h with 1μM Etop or Doxo, lysed and analyzed. Shown is the quantification of broken DNA relative to input. (B) Western blotting analysis for γ-H2AX. Cells were treated with 1μM Etop for 1h, washed and lysed at the indicated time points. Right panel: quantification of the signals detected on the WB. Signals were normalized to actin and t=0 was set at 1. (C) GFP or GFP-C9orf82 over-expressing MelJuSo cells were exposed to 5μM Etop and analyzed for γ-H2AX as in (B). (D) MelJuSo cells stably over-expressing GFP or GFP-C9orf82 were treated with 1μM Etop for 2h. Drugs were removed before further culture. Cells were lysed at the indicated time points post drug removal. DNA break repair was analyzed using constant field gel electrophoresis. Lower band represents the broken DNA and the top band the intact DNA. Separate panels are different cut-outs from the same gel. For quantification, t=0 of the GFP or GFP-C9orf82 cells was set at 1. (E) Cellular localization of C9orf82 by confocal imaging of MelJuSo cells stably expressing GFP-C9orf82 and stained for DAPI (blue) and actin (red). Scale bar: 10μm. All experiments shown are mean ± SD of three independent experiments. Statistical significance compared to control (* p < 0.05, ** p < 0.01). NT = non-treated.*

generated C9orf82 knockout clone (Figure S3A-C). Conversely, ectopic expression of GFP-tagged C9orf82 in MelJuSo melanoma cells (a cell line with fast DNA repair kinetics) led to a stronger and more persistent γ-H2AX DNA damage response upon Etop treatment (Figure 4C). Since DNA repair already takes place during the first hour of Etop treatment, these data indicate that C9orf82 influences the kinetics of γ-H2AX resolution and hereby the DNA damage response. To assess whether C9orf82 regulates DSB repair itself, we determined the DSB repair kinetics in cells overexpressing either GFP or GFP-C9orf82 (Figure 4D), with the latter resulting in decreased Etop-induced DNA DSB repair. This suggests that C9orf82 decreases the rate of DNA repair.

Although C9orf82 localizes primarily in the nucleus (Figure 4E), it is unlikely to directly inhibit DNA repair, since it is not recruited to Etop-induced γ-H2AX foci (Figure S3D). On this basis, C9orf82 appears to attenuate DNA double-strand break repair induced by Topo II poisons, for its loss serves to accelerate DNA damage repair, thereby promoting resistance to DNA double-strand break inducers such as Doxo and Etop. The exact molecular mechanism of DNA repair modulation by this novel protein is at present unclear.

The SWI/SNF complex controls chromatin loading of Topo II to confer drug resistance

In addition to the resistance factors described above, we also identified two subunits of the SWI/SNF complex involved in the resistance to Topo II poisons. The SWI/SNF complex is known to modulate transcription through chromatin remodeling [18]. Additionally, it has recently been shown to mediate decatenation of chromatids during mitosis by loading Topo IIα onto the DNA [26]. The latter suggests a possible means by which the SWI/SNF complex may affect the susceptibility of cells to Topo II poisons, by reducing the chromatin loading and activity of Topo IIα. To address this, HAP1 cells either proficient in or depleted of the SWI/SNF subunit SMARCB1 were exposed to Etop or Doxo, and the resulting DNA double-strand breaks were quantified. The SMARCB1-depleted cells exhibited significantly lower levels of such DNA breaks (Figure 5A), as well as reduced DNA damage response signaling, as visualized by γ-H2AX analysis (Figure 5B and 5C). These changes were not a result of drug uptake deficiency (Figure 5D) or altered expression levels of Topo IIα (Figure 5E). Given that SMARCB1 interacts with Topo IIα (Figure 5F) [26], the expected reduction in loading of Topo IIα onto the DNA in cells compromised for SMARCB1 presents a likely explanation for the diminished efficacy of Topo II poisons in these cells. To confirm this, we assessed the association of Topo IIα to the chromatin using a chromatin binding assay as described in [26]. Treatment of cells with Etop yielded more Topo IIα loaded onto chromatin (Figure 4G), indicating this assay can be used to assess Topo IIα activity and arrest. In line with our hypothesis, SMARCB1 depletion resulted in a decreased amount of Topo IIα loaded onto chromatin after Etop exposure (Figure 4G), indicating that loss of SMARCB1 reduces the level of Topo IIα that is poisoned on the chromatin. These results suggest that the SWI/SNF complex modulates resistance to TopoII poisons by controlling the loading of Topo IIα onto the DNA.

Expression of SWI/SNF subunits in epithelioid sarcoma and triple negative breast cancers correlate to doxorubicin response

Although mutations in the SWI/SNF members are frequently observed in human tumors [14], their relationship to clinical outcome is lacking. Epithelioid sarcomas
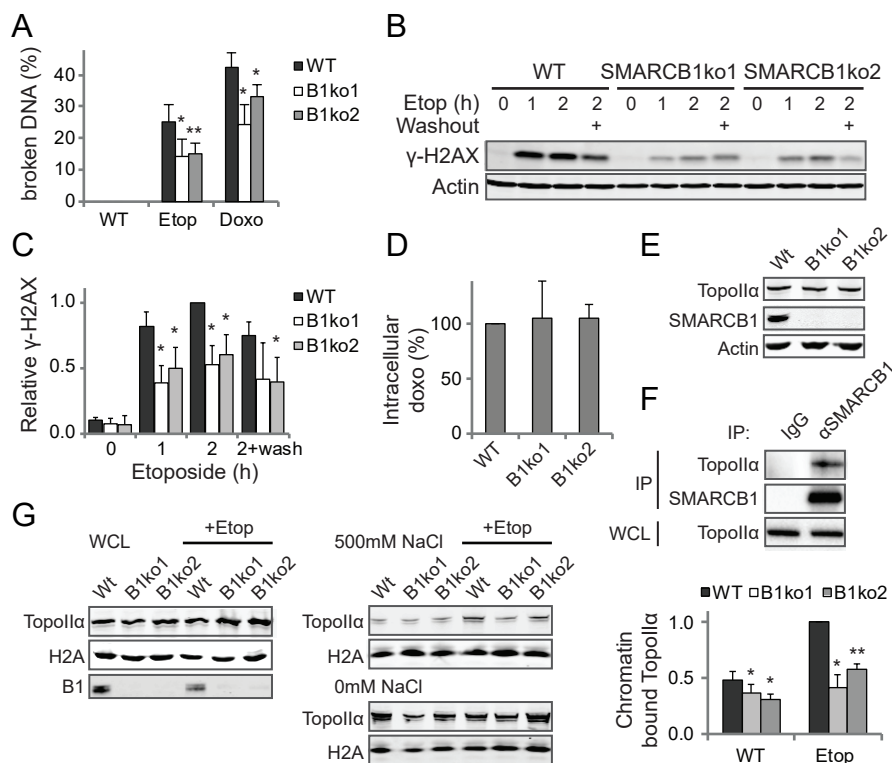
Figure 5. The SWI/SNF complex regulates Topo IIα chromatin loading and activity. *(A) The amount of Etop- or Doxo-induced DNA breaks was quantified by constant field gel electrophoresis. HAP1 WT and SMARCB1 knockout cells were treated for 2h with 1μM Etop or Doxo. Shown is the quantification of the relative amount of broken DNA. (B) Western blot analysis for γ-H2AX after exposing cells to 5μM Etop for the indicated time points, or first treated for 2h and lysed 2h (lanes '+') after Etop removal. Actin is probed as a loading control. (C) Quantification of (B). The γ-H2AX signal is normalized to the actin signal and t=2 hours for WT is set at 1. (D) Quantification of Doxo uptake levels by flow cytometry. The different cells were incubated for 1h with 2μM Doxo before analysis. (E) Western blot analysis of Topo IIα expression levels in HAP1 cells either or not depleted for SMARCB1, as indicated. Actin is shown as loading control. (F) Co-immunoprecipitation (IP) of SMARCB1 and Topo IIin HAP1 cells followed by SDS-PAGE and Western blotting. IgG IP is used as control. WCL: Topo II in total lysates are shown as loading control. (G) Chromatin association assay for TopoIIα. Chromatin pellets of indicated HAP1 cells untreated or treated with 1μM Etop for 15min were lysed directly (WCL), or treated with the indicated salt concentration (0mM or 500mM) before lysis. For quantification, the 500mM NaCl Topo IIα signal was corrected for loading (H2A) and WCL input signal. WT Etop 15 min was set at 1. All experiments shown are mean ± SD of independent triplicates. Statistical significance was calculated compared to control (* $p < 0.05$, ** $p < 0.01$).*

are known to harbor deletions of the SMARCB1 gene in 60-90% of the cases [27, 28] and are commonly treated with Doxo-containing regimens. Re-analysis of a previously reported dataset [28] revealed that patients with a deletion for SMARCB1 experienced more relapses after treatment (Figure 6A), suggesting a relationship between SMARCB1 expression and treatment outcome. To further assess whether SWI/SNF status correlates directly with patient responses to treatment with Topo II
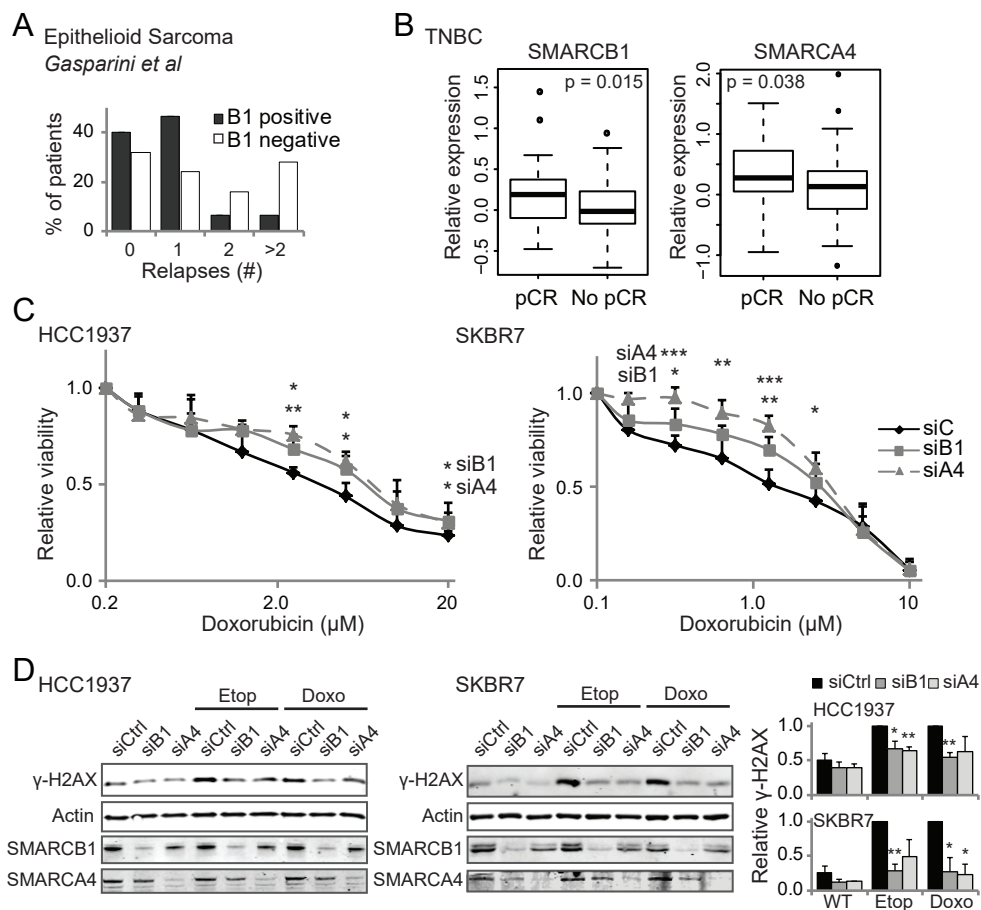
Figure 6. SMARCB1 and SMARCA4 expression correlates to responses to Doxo in triple negative breast cancer cells and patients. *(A) Re-analysis of the number of relapses in 25 SMARCB1 negative and 15 SMARCB1 positive epithelioid sarcoma patients, as described in [28]. (B) Box plot representing the expression of SMARCB1 and SMARCA4 in 113 triple-negative breast cancer patients with a pathological complete response (pCR, 46 patients) or not (no pCR, 67 patients) following a Doxo containing regimen. Statistical significance was calculated using a Student's T-test. (C) HCC1937 or SKBR7 cells were transfected with control siRNAs or siRNAs targeting SMARCB1 or SMARCA4. 72h after transfection, cells were treated with the indicated doses of Doxo for 2h and cell viability was analyzed 72h after drug exposure. (D) HCC1937 or SKBR7 cells were transfected with siRNAs as in (C) and treated 72h later with 5µM Etop or Doxo for 1h, lysed and analyzed with SDS-PAGE and western blotting analysis. Quantifications in (C-D) are mean ± SD of independent triplicate experiments. Statistical significance was calculated compared to control (* p < 0.05, ** p < 0.01, *** p < 0.001).*

poisons, we used an expression dataset of 116 human triple-negative breast cancer (TNBC) patients treated at our cancer center with a regimen of Doxo and cyclophosphamide. We compared the expression of the SWI/SNF complex subunits SMARCB1, SMARCA4, SMARCE1 and ARID1a with the clinical response to this treatment. Our analysis showed that patients with a pathological complete response had a significantly higher expression of SMARCB1 and SMARCA4 (Figure 6B), but

not ARID1a or SMARCE1 (Figure S4A). Furthermore, by analyzing the other genes identified from the screen, we found a significant correlation between response and expression for Keap1, but not C9orf82 (Figure S4A). These data suggest that in triple-negative breast cancer patients, low expression of SMARCB1 and SMARCA4 is associated with poor response to a Doxo-containing regimen.

To validate that SMARCB1 and SMARCA4 causally regulate sensitivity to Doxo in TNBC settings, we silenced both genes in two TNBC cell lines, HCC1937 and SKBR7 (Keap1 silencing was toxic for these cells and could not be tested). Silencing of both genes rendered cells more resistant to Doxo (Figure 6C) and led to a reduced induction of DNA damage signaling (Figure 6D). Taken together, loss or reduced expression of SMARCB1 and SMARCA4 negatively impacts Doxo-induced DNA double-strand break formation and leads to drug resistance in triple negative breast cancer cell lines and patients.

DISCUSSION

Annually, nearly 1 million cancer patients are treated with Topo II poisons such as Doxo, Daun or Etop. Yet, resistance to these drugs persists as a major complication in cancer treatment. Because the molecular basis for this resistance is not fully understood, many patients receive ineffective treatments accompanied by adverse side effects in the absence of the corresponding clinical benefit [1]. To facilitate treatment outcome predictions for Doxo relative to other available alternative drugs, improved insights into the mechanisms of drug resistance are necessary. Using a genome-wide screening approach, we identified and characterized several novel factors involved in resistance to Topo II poisons. In addition to the previously described factors, including the drug transporter ABCB1 and adaptor Keap1, we identified C9orf82 and the SWI/SNF complex as novel regulators of Doxo resistance. Keap1, C9orf82 and SWI/SNF can all be placed in the pathway involving Topo II-induced DNA double-strand break formation and the subsequent DDR (Figure 7). Consequently, depletion
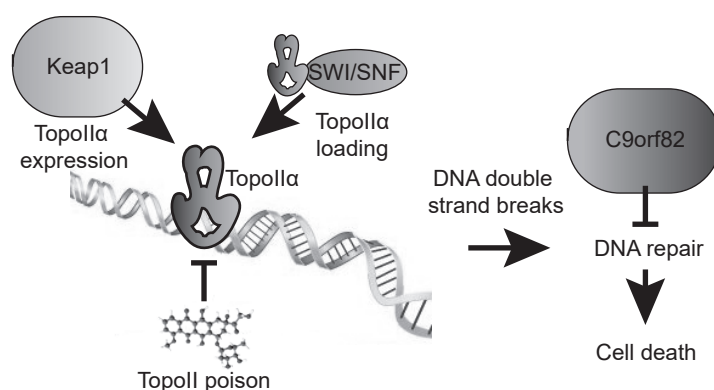

Figure 7. Model of SWI/SNF, Keap1 and C9orf82 regulating different phases of Topo II poison-induced DNA break formation and DDR. *Topo II poisons like Doxo induce DNA double-strand breaks by trapping Topo II on the DNA. If not sufficiently repaired, this leads to cell death. Keap1 controls the expression of Topo IIα, while SWI/SNF regulates the loading and hereby activity of Topo IIα. Loss of these genes therefore attenuates DNA double-strand break formation by Topo II poisons. In the next phase of the DNA breaks and repair cycle, C9orf82 controls DNA repair. Loss of C9orf82 accelerates DNA repair, reducing cell death induced by Topo II poisons.*

of these genes does not confer resistance to either the Topo I inhibitor TPT, or Acla, an anthracycline that does not induce DNA double-strand breaks [3].

Keap1 has already been studied in the context of chemosensitivity to several classes of anti-cancer drugs, including alkylating agents, anti-mitotic agents and Topo II poisons [11, 17, 21]. Inhibition of its cognate substrate Nrf2 sensitizes cells to a number of these drugs, suggesting that Keap1 influences sensitivity by virtue of Nrf2 destabilization [11, 17]. However, Keap1 controls several other signaling pathways [29-31], and could thus affect drug resistance in other ways. We interrogated these two options by depleting Nrf2 and found that asides from regulating Nrf2, Keap1 induces resistance to Topo II poisons by controlling the expression levels of Topo IIα. Clinically, we show that the expression of Keap1 is correlated to the response of triple negative breast cancer patients to Doxo and cyclophosphamide. Keap1 inactivating mutations and deletions are frequently observed in human tumors [32, 33]. For example, 12-15% of lung tumors have inactivated Keap1 [32] and since these tumors are frequently treated with combinations of Etop and cisplatin, it may be beneficial to determine patients' Keap1 mutational status to assess the proper treatment protocol.

We also defined C9orf82 as a novel factor involved in resistance to Topo II poisons, most notably Etop. A previous study has identified C9orf82 as a negative regulator of caspase-mediated apoptosis [25], which is not in line with our observations that C9orf82 depletion desensitizes cells to Etop. Our data indicate that C9orf82 is a nuclear protein that controls the rate of DNA double-strand break repair after exposure to Topo II poisons. Doxo itself slows down DNA repair, which might explain why the resistance is most prominent following Etop exposure. Given that most Etop-induced DNA double-strand breaks are repaired by non-homologous end-joining (NHEJ) [34], C9orf82 may impinge on this arm of the DNA repair pathway, but how is currently unclear. C9orf82 is found mutated in 7-11% of glioblastoma tumors [13, 35], which makes it a potential prognostic factor in the treatment of such patients with Etop. However, further studies integrating clinical response data with mutational analyses are required to substantiate this possibility.

Besides this relatively unknown protein, we characterized the role of the SWI/SNF complex in the resistance to TopoII poisons. The SWI/SNF complex is mutated in around 20% of human tumors [14] and has been linked to tumor suppression [26]. SWI/SNF complex subunits like SMARCB1 control the loading of Topo IIα onto the DNA and hereby determine the extent of DNA damage induced following exposure to Topo II poisons. SMARCB1 depleted cells therefore have less DNA breaks when exposed to Topo II poisons and thus a growth advantage. As many of the tumors that harbor mutations in the SWI/SNF complex are treated with Topo II poisons, drug-resistance could arise even when Topo IIα is expressed.

Several lines of evidence support this notion in patients. For example, SMARCB1 is mutated in 90-100% of the rhabdoid tumors [36, 37], a very aggressive childhood tumor that is unresponsive to Doxo [38]. Also, epithelioid sarcoma patients harboring deletions for SMARCB1 have a higher chance of relapse following treatment protocols that usually includes Topo II poisons [28]. Furthermore, we explored a data set of triple negative breast cancer patients where both gene expression and treatment responses were documented. A correlation between treatment response and expression of SWI/SNF subunits SMARCB1 and SMARCA4 was observed within patients treated with Doxo and cyclophosphamide. No correlation was observed for SMARCE1 and ARID1a, which could be because SMARCE1 is not a part of the core complex essential for activity and ARID1a has redundancy with ARID1b [18], or because the expression of these factors is not the limiting factor for the complex

to function. Given the resistance to Doxo observed in our cell culture experiments, these data suggest that patients with low or depleted SWI/SNF expression should not be treated with Doxo, but rather with Acla or TPT, which are drugs that work through a different mechanism and that do not show any cross-resistance in our experiments.

In conclusion, we identified and characterized three factors controlling sensitivity to the frequently used anti-cancer drugs Doxo and Etop. Keap1, C9orf82 and the SWI/SNF chromatin remodeling complex all act by affecting DNA double-strand break formation or repair following exposure to these drugs. Mutations in these genes are frequently observed in human tumors and expected to yield tumors that are resistant to these drugs, as we show for triple negative breast cancer patients. Profiling patients for mutations in these genes can further stratify treatment options as non-responding patients can be selected for other treatments rather than given ineffective treatment containing Topo II poisons.

MATERIALS AND METHODS
Cell culture and constructs
HAP1 and MelJuSo cells were grown in IMDM supplemented with 8% FCS. SKBR7 and HCC1937 cells were grown in RPMI with 8% FCS. HAP1 cells were generated as described in [39], sequence verified during the screen and kept under low passage afterwards. MelJuSo cells were initially described in [40] and sequence verified in 2013 [3], since then identity was confirmed by staining for marker MHCII. HCC1937 cells were obtained from ATCC (www.ATCC.org), where they were validated using STR profiling, and kept under low passage after receipt. SKBR7 cells were a kind gift from Klaas de Lint (Netherlands Cancer Institute, division of Molecular Carcinogenesis) and analyzed using STR profiling in 2015. Keap1 knockdown cells were generated by transduction with lentiviral vectors containing an shRNA sequence targeting Keap1. Keap1 sh1 targeted the 5'-GCGAATGATCACAGCAAT-GAA-3' sequence of Keap1 and Keap1 sh2 the 5'-CGGGAGTACATCTACATGCAT-3' sequence. Cells were maintained under puromycin (2.5 µg/ml) selection to generate stable knockdown cells. For GFP-C9orf82, the sequence of full length C9orf82 was cloned from an Image clone (#4648932) into the mGFP-C1 vector (Clontech) using the primers 5'-CCCAAAGCTTCCATGACGGGGAAAAAGTCCTC-3' and 5'-CCCAG-GTACCCTAGGCTGGCTTTTTTATATC-3'. MelJuSo cells were transfected using effectene (Qiagen) and cells expressing GFP or GFP-C9orf82 were maintained under continuous selection with G418 (200 µg/ml).

Haploid genetic screen
The haploid genetics screen was performed as described [10]. In brief, gene trap virus was produced by transfecting the gene-trap plasmid together with packaging plasmids in HEK 293T cells. Virus was harvested, concentrated, and used to infect 1×10^8 HAP1 cells. After brief passaging to allow for protein turnover, mutagenized cells were exposed to the doxorubicin regimen described below. Drug resistant cells were expanded, genomic DNA was isolated and subsequently retroviral insertion sites were amplified by inverse PCR and mapped by parallel sequencing (Illumina HiSeq2000) of the genomic inserts. The enrichment of insertions in the drug-treated group was calculated by comparing the number of insertions between the doxorubicin-treated group and an unselected population [39] using a one-sided Fisher's exact test. These values were corrected for false discovery rate using the Benjamini and Hochberg method [10].

Generation of null alleles using CRISPR-Cas9

CRISPR targeting sequences were designed based on the tool from crispr.mit.edu [41]. Oligo's were cloned into the pX330 backbone [42] and transfected using effectene (Qiagen) together with a vector containing a guide RNA to the zebrafish TIA gene (5'-ggtatgtcgggaacctctcc-3') and a blasticidin resistance gene with a 2A sequence that is flanked by two TIA target sites. Cells positive for both vectors excise the blasticidin resistance gene from the vector and will sporadically incorporate it into the targeted genomic locus by non-homologous end-joining [43]. Successful integration of the cassette into the targeted gene disrupts the allele and renders cells resistant to blasticidin. The targeting sequences were: SMARCB1: KO1, 5'-TG-GCGCTGAGCAAGACCTTC-3' and KO2, 5'-TGGCGCTGAGCAAGACCTTC-3', C9orf82: KO1, 5'-CAACGCGGGTACGATGTCCG-3' and KO2, 5'-TGACGGG-GAAAAAGTCCTCC-3', and Nrf2: 5'-TGGAGGCAAGATATAGATCT-3'. Cells were selected on blasticidin (10μg/ml) for two days and knockout clones were validated by sequencing the genomic DNA. The following primers were used to detect deletion at the genomic level: SMARCB1 fw: 5'-CATTTCGCCTTCCGGCTTCGG-3', SMARCB1 rv: 5'-CTCGGAGCCGATCATGTAGAACTC-3', C9orf82 fw: 5'-GGAAGTGACG-CATAACCTGCGAC-3', C9orf82 rv: 5'-CTGCAAGGAGCCCGAGACG-3', Nrf2 fw: 5'-GACATGGATTTGATTGACATACTTTGGAGGC-3', Nrf2 rv: 5'-CTGACTGGAT-GTGCTGGGCTGG-3'.

Reagents and siRNA transfections

Doxorubicin, etoposide and topotecan were obtained from Pharmachemie and daunorubicin was obtained from Sanofi-Aventis. Aclarubicin was obtained from Santa Cruz. Antibodies used for IP, Western blot and microscopy: mouse anti-Keap1, mouse anti-tubulin, mouse anti-actin (all from Sigma), rabbit anti-Topoisomerase II, rabbit anti-SMARCB1, rabbit anti-SmarcA4, rabbit anti-SMARCE1, rabbit anti-ARID1a (all from Bethyl laboratories), mouse anti-γH2AX, rabbit anti-H2A (Millipore). For siRNA mediated depletion of SMARCA4 and SMARCB1, cells were reverse transfected with DharmaFECT transfection reagent #1 and 50 nM siRNA (Human siGenome SMARTpool, Dharmacon) according to the manufacturing protocol. Briefly, siRNAs and DharmaFECT were mixed and incubated for 20 minutes, after which cells were added and left to adhere. Three days later, cells were treated and lysed for SDS-PAGE and Western blotting analysis or left to grow out for three more days for the cell viability assay.

Long-term proliferation assays

Cells were seeded into 12-well plates (5000 cells per well). The next day, drugs were added at concentrations indicated and cultured for two hours. Subsequently, drugs were removed and cells were left to grow for 7-9 days, fixed using 3.7% formaldehyde and stained using 0.1% Crystal violet solution (Sigma). Quantification of colonies was done by Image J.

Short-term growth inhibition assays

Cells were seeded into 96-well plates (2000 cells per well) and exposed the next day to the indicated drugs (for siRNA knockdowns, cells were seeded three days before treatment). Drugs were removed two hours later and cultured for an additional 72 hours. Cell viability was measured using the Cell Titer Blue viability assay (Promega). Relative survival was normalized to the untreated control and corrected for background signal.

Co-immunoprecipitation and Western blotting
For co-immunoprecipitation experiments of nuclear proteins, cells were trypsinized, counted and lysed (25mM HEPES pH 7.6, 5mM $MgCl_2$, 25mM KCl, 0.05mM EDTA, 10% glycerol and 0.1% NP-40 supplemented with complete EDTA-free Protease Inhibitor Cocktail (Roche)). Nuclei were isolated by spinning at 1,300 g and subsequently sonicated for 30 minutes in lysis buffer (50 mM Tris-HCl, pH 8.0, 150 mM NaCl, 0.1% NP-40 supplemented with Protease Inhibitor Cocktail (Roche)). Chromatin was removed by centrifugation (5 min at 12,000 g) and the supernatant was pre-cleared with protein G dynabeads (Life Technologies). Lysate was incubated overnight with 3µg antibody and 20µl protein G Dynabeads. Beads were washed extensively and re-suspended in SDS-sample buffer (2% SDS, 10% glycerol, 5% β-mercaptoethanol, 60mM Tris-HCl pH 6.8 and 0.01% bromophenol blue) before analysis by SDS-PAGE.

For whole cell lysate analyses, cells were lysed directly in SDS sample buffer (2% SDS, 10% glycerol, 5% β-mercaptoethanol, 60mM Tris-HCl pH 6.8 and 0.01% bromophenol blue). Samples were analyzed by SDS-PAGE and Western blotting. Blocking of the filter and antibody incubations were done in PBS supplemented with 0.1 (v/v)% Tween and 5% (w/v) bovine milk powder.

Constant-field gel electrophoresis
DNA double-strand breaks were quantified by constant-field gel electrophoresis as described [44]. In short, HAP1 cells were treated with Doxo or Etop for two hours. Drugs were removed and cells were lysed and processed immediately to isolate the DNA. Samples were separated on a 0.8% agarose gel to separate faster migrating broken DNA from intact DNA and fragments of over >1 MB. Images were analyzed by ImageJ.

Flow cytometry
Cells were treated with Doxo (2µM) for one hour and trypsinized and fixed with 3.7% formaldehyde. Fluorescence of Doxo was measured directly using a FACSCalibur flow cytometer (BD Bioscience) and further analyzed by FlowJo software.

cDNA synthesis and qPCR
RNA isolation, cDNA synthesis and quantitative RT-PCR were performed as described previously [45]. The primers for detection of Keap1, NQO1 and GAPDH expression were: Keap1 fw: 5'-CTGGAGGATCATACCAAGCAGG-3', Keap1 rv: 5'-GAACATG-GCCTTGAAGACAGG-3', NQO1 fw: 5'-GGGCAAGTCCATCCCAACTG-3', NQO1 rv: 5'-GCAAGTCAGGGAAGCCTGGA-3', GAPDH fw: 5'-TGTTGCCATCAATGACC-CCTT-3', GAPDH rv: 5'-CTCCACGACGTACTCAGCG-3'.

Confocal microscopy
MelJuSo cells were seeded on coverslips and treated as indicated in the respective experiments. Cells were fixed in 3.7% formaldehyde for 10 min and permeabilized by 0.1% Triton X-100. Staining was performed with the antibodies mentioned above or with phalloidin (Invitrogen) to stain F-actin and DAPI (Invitrogen) to stain DNA. Images were acquired using a Leica TCS SP5 confocal microscope.

Chromatin association assay
HAP1 cells were seeded and treated with Etop for 15 min before lysis when indicated. Cells were lysed in lysis buffer (25 mM HEPES pH7.6, 5mM $MgCl_2$, 25mM

2

KCl, 0.05mM EDTA, 10% glycerol, 0.1% NP-40) and nuclei were spun down and re-suspended at a concentration of 60 million/ml in buffer (20mM Tris-HCl pH 7.6, 3mM EDTA). 25ul samples were adjusted to the indicated NaCl concentrations to a total volume of 50ul. After mixing and incubation on ice for 20 min, chromatin was spun down and re-suspended in sample buffer. After sonication, samples were analyzed by SDS-PAGE and Western blotting.

Gene expression analysis of the neoadjuvant breast cancer cohort
Gene expression data was obtained from 113 pre-treatment biopsies of triple nega-tive breast cancer patients treated at the Antoni van Leeuwenhoek hospital (associ-ated to the NKI) and scheduled to receive neoadjuvant chemotherapy. All patients had a breast carcinoma with either a primary tumor size of at least 3 cm, or the presence of axillary lymph node metastases. A treatment regimen was assigned to each patient, consisting of six courses of dose-dense doxorubicin/cyclophospha-mide (ddAC). If the therapy response was considered unfavorable by MRI evaluation after three courses, ddAC was changed to capecitabine/docetaxel (XD). Response to therapy was defined as pathological complete response (pCR) or no pathological complete response at the time of surgery. 63 samples were labeled and hybrid-ized to Illumina 6v3 arrays (Illumina, La Jolla, CA). Data were log2 transformed and between-array normalized using simple scaling. When a single gene was repre-sented by multiple probes, the probe with the highest variance was chosen. The data is made available through the GEO database, accession GSE34138 (http://www.ncbi.nlm.nih.gov/geo/query/acc.cgi?acc=GSE34138) [46]. 50 samples were profiled using RNAseq. Strand-specific sequencing libraries were generated using the TruSeq Stranded mRNA sample preparation guide (Illumina Part # 15031047 Rev. E) according to the manufacturer's instructions. Deep Sequencing was done with a HiSeq2000 machine (Illumina Inc). The reads are mapped against the hu-man reference (hg19) using Tophat (version 2.0.6) [47]. Tophat was supplied with a known set of genemodels using a GTF file (Ensembl version 66). HTSeq-count [48] was used to define gene expressions. This tool generates a list of the total number of uniquely mapped reads for each gene that was provided in the GTF. These data were normalized based on the relative library size using the DESeq2 R package [49] and subsequently log transformed.

Statistical methods
All experiments were performed at least three times in an independent manner. All data are presented as means ± SD. The results were analyzed by using a paired two-tailed Student's T-test (unpaired for the data in Figure 6B). Significance was calculated using Excel and defined as $p < 0.05$.

REFERENCES
1. Pommier, Y. (2013) Drugging topoisomerases: lessons and challenges, ACS chemical biology. 8, 82-95.
2. Borst, P. (2012) Cancer drug pan-resistance: pumps, cancer stem cells, quiescence, epithelial to mesenchymal transition, blocked cell death pathways, persisters or what?, Open biology. 2, 120066.
3. Pang, B., Qiao, X., Janssen, L., Velds, A., Groothuis, T., Kerkhoven, R., Nieuwland, M., Ovaa, H., Rottenberg, S., van Tellingen, O., Janssen, J., Huijgens, P., Zwart, W. & Neefjes, J. (2013) Drug-induced histone eviction from open chromatin contributes to the chemotherapeutic effects of doxorubicin, Nat Commun. 4, 1908.
4. Yang, F., Kemp, Christopher J. & Henikoff, S. (2013) Doxorubicin Enhances Nucleosome Turnover around Promoters, Current Biology. 23, 782-787.
5. Pang, B., de Jong, J., Qiao, X., Wessels, L. F. & Neefjes, J. (2015) Chemical profiling of the genome with anti-cancer drugs defines target specificities, Nature chemical biology.
6. Callaghan, R., Luk, F. & Bebawy, M. (2014) Inhibition of the multidrug resistance P-glycoprotein: time for a change of strategy?, Drug metabolism and disposition: the biological fate of chemicals. 42, 623-31.
7. Burgess, D. J., Doles, J., Zender, L., Xue, W., Ma, B., McCombie, W. R., Hannon, G. J., Lowe, S. W. & Hemann, M. T. (2008) Topoisomerase levels determine chemotherapy response in vitro and in vivo, Proceedings of the National Academy of Sciences of the United States of America. 105, 9053-8.
8. Bouwman, P. & Jonkers, J. (2012) The effects of deregulated DNA damage signalling on cancer chemotherapy response and resistance, Nature reviews Cancer. 12, 587-98.
9. Zoppoli, G., Regairaz, M., Leo, E., Reinhold, W. C., Varma, S., Ballestrero, A., Doroshow, J. H. & Pommier, Y. (2012) Putative DNA/RNA helicase Schlafen-11 (SLFN11) sensitizes cancer cells to DNA-damaging agents, Proceedings of the National Academy of Sciences of the United States of America. 109, 15030-5.
10. Carette, J. E., Guimaraes, C. P., Wuethrich, I., Blomen, V. A., Varadarajan, M., Sun, C., Bell, G., Yuan, B., Muellner, M. K., Nijman, S. M., Ploegh, H. L. & Brummelkamp, T. R. (2011) Global gene disruption in human cells to assign genes to phenotypes by deep sequencing, Nature biotechnology. 29, 542-6.
11. Shibata, T., Kokubu, A., Gotoh, M., Ojima, H., Ohta, T., Yamamoto, M. & Hirohashi, S. (2008) Genetic alteration of Keap1 confers constitutive Nrf2 activation and resistance to chemotherapy in gallbladder cancer, Gastroenterology. 135, 1358-1368, 1368.e1-4.
12. Singh, A., Misra, V., Thimmulappa, R. K., Lee, H., Ames, S., Hoque, M. O., Herman, J. G., Baylin, S. B., Sidransky, D., Gabrielson, E., Brock, M. V. & Biswal, S. (2006) Dysfunctional KEAP1-NRF2 interaction in non-small-cell lung cancer, PLoS medicine. 3, e420.
13. Network, C. G. A. R. (2008) Comprehensive genomic characterization defines human glioblastoma genes and core pathways, Nature. 455, 1061-8.

14. Kadoch, C., Hargreaves, D. C., Hodges, C., Elias, L., Ho, L., Ranish, J. & Crabtree, G. R. (2013) Proteomic and bioinformatic analysis of mammalian SWI/SNF complexes identifies extensive roles in human malignancy, Nature genetics. 45, 592-601.

15. Benjamin, R. S., Riggs, C. E., Jr. & Bachur, N. R. (1977) Plasma pharmacokinetics of adriamycin and its metabolites in humans with normal hepatic and renal function, Cancer research. 37, 1416-20.

16. Ohta, T., Iijima, K., Miyamoto, M., Nakahara, I., Tanaka, H., Ohtsuji, M., Suzuki, T., Kobayashi, A., Yokota, J., Sakiyama, T., Shibata, T., Yamamoto, M. & Hirohashi, S. (2008) Loss of Keap1 function activates Nrf2 and provides advantages for lung cancer cell growth, Cancer research. 68, 1303-9.

17. Wang, X. J., Sun, Z., Villeneuve, N. F., Zhang, S., Zhao, F., Li, Y., Chen, W., Yi, X., Zheng, W., Wondrak, G. T., Wong, P. K. & Zhang, D. D. (2008) Nrf2 enhances resistance of cancer cells to chemotherapeutic drugs, the dark side of Nrf2, Carcinogenesis. 29, 1235-43.

18. Hohmann, A. F. & Vakoc, C. R. (2014) A rationale to target the SWI/SNF complex for cancer therapy, Trends in genetics : TIG. 30, 356-63.

19. Tsang, W. P., Chau, S. P., Kong, S. K., Fung, K. P. & Kwok, T. T. (2003) Reactive oxygen species mediate doxorubicin induced p53-independent apoptosis, Life sciences. 73, 2047-58.

20. Rogalska, A., Koceva-Chyla, A. & Jozwiak, Z. (2008) Aclarubicin-induced ROS generation and collapse of mitochondrial membrane potential in human cancer cell lines, Chemico-biological interactions. 176, 58-70.

21. Konstantinopoulos, P. A., Spentzos, D., Fountzilas, E., Francoeur, N., Sanisetty, S., Grammatikos, A. P., Hecht, J. L. & Cannistra, S. A. (2011) Keap1 mutations and Nrf2 pathway activation in epithelial ovarian cancer, Cancer research. 71, 5081-9.

22. Sporn, M. B. & Liby, K. T. (2012) NRF2 and cancer: the good, the bad and the importance of context, Nature reviews Cancer. 12, 564-71.

23. Miyoshi, Y., Kurosumi, M., Kurebayashi, J., Matsuura, N., Takahashi, M., Tokunaga, E., Egawa, C., Masuda, N., Kono, S., Morimoto, K., Kim, S. J., Okishiro, M., Yanagisawa, T., Ueda, S., Taguchi, T., Tamaki, Y. & Noguchi, S. (2010) Predictive factors for anthracycline-based chemotherapy for human breast cancer, Breast cancer (Tokyo, Japan). 17, 103-9.

24. Sinha, B. K., Haim, N., Dusre, L., Kerrigan, D. & Pommier, Y. (1988) DNA strand breaks produced by etoposide (VP-16,213) in sensitive and resistant human breast tumor cells: implications for the mechanism of action, Cancer research. 48, 5096-100.

25. Zhang, Y., Johansson, E., Miller, M. L., Janicke, R. U., Ferguson, D. J., Plas, D., Meller, J. & Anderson, M. W. (2011) Identification of a conserved anti-apoptotic protein that modulates the mitochondrial apoptosis pathway, PloS one. 6, e25284.

26. Dykhuizen, E. C., Hargreaves, D. C., Miller, E. L., Cui, K., Korshunov, A., Kool, M., Pfister, S., Cho, Y. J., Zhao, K. & Crabtree, G. R. (2013) BAF complexes facilitate decatenation of DNA by topoisomerase IIalpha, Nature. 497, 624-7.

27. Hornick, J. L., Dal Cin, P. & Fletcher, C. D. (2009) Loss of INI1 expression is characteristic of both conventional and proximal-type epithelioid sarcoma, The American journal of surgical pathology. 33, 542-50.

28. Gasparini, P., Facchinetti, F., Boeri, M., Lorenzetto, E., Livio, A., Gronchi, A., Ferrari, A., Massimino, M., Spreafico, F., Giangaspero, F., Forni, M., Maestro, R., Alaggio, R., Pilotti, S., Collini, P., Modena, P. & Sozzi, G. (2011) Prognostic determinants in epithelioid sarcoma, European journal of cancer (Oxford, England : 1990).

47, 287-95.

29. Lee, D. F., Kuo, H. P., Liu, M., Chou, C. K., Xia, W., Du, Y., Shen, J., Chen, C. T., Huo, L., Hsu, M. C., Li, C. W., Ding, Q., Liao, T. L., Lai, C. C., Lin, A. C., Chang, Y. H., Tsai, S. F., Li, L. Y. & Hung, M. C. (2009) KEAP1 E3 ligase-mediated downregulation of NF-kappaB signaling by targeting IKKbeta, Molecular cell. 36, 131-40.

30. Fan, W., Tang, Z., Chen, D., Moughon, D., Ding, X., Chen, S., Zhu, M. & Zhong, Q. (2010) Keap1 facilitates p62-mediated ubiquitin aggregate clearance via autophagy, Autophagy. 6, 614-21.

31. Zhan, L., Zhang, H., Zhang, Q., Woods, C. G., Chen, Y., Xue, P., Dong, J., Tokar, E. J., Xu, Y., Hou, Y., Fu, J., Yarborough, K., Wang, A., Qu, W., Waalkes, M. P., Andersen, M. E. & Pi, J. (2012) Regulatory role of KEAP1 and NRF2 in PPAR-gamma expression and chemoresistance in human non-small-cell lung carcinoma cells, Free radical biology & medicine. 53, 758-68.

32. Lawrence, M. S., Stojanov, P., Mermel, C. H., Robinson, J. T., Garraway, L. A., Golub, T. R., Meyerson, M., Gabriel, S. B., Lander, E. S. & Getz, G. (2014) Discovery and saturation analysis of cancer genes across 21 tumour types, Nature. 505, 495-501.

33. Barbano, R., Muscarella, L. A., Pasculli, B., Valori, V. M., Fontana, A., Coco, M., la Torre, A., Balsamo, T., Poeta, M. L., Marangi, G. F., Maiello, E., Castelvetere, M., Pellegrini, F., Murgo, R., Fazio, V. M. & Parrella, P. (2013) Aberrant Keap1 methylation in breast cancer and association with clinicopathological features, Epigenetics : official journal of the DNA Methylation Society. 8, 105-12.

34. Quennet, V., Beucher, A., Barton, O., Takeda, S. & Lobrich, M. (2011) CtIP and MRN promote non-homologous end-joining of etoposide-induced DNA double-strand breaks in G1, Nucleic acids research. 39, 2144-52.

35. Brennan, C. W., Verhaak, R. G., McKenna, A., Campos, B., Noushmehr, H., Salama, S. R., Zheng, S., Chakravarty, D., Sanborn, J. Z., Berman, S. H., Beroukhim, R., Bernard, B., Wu, C. J., Genovese, G., Shmulevich, I., Barnholtz-Sloan, J., Zou, L., Vegesna, R., Shukla, S. A., Ciriello, G., Yung, W. K., Zhang, W., Sougnez, C., Mikkelsen, T., Aldape, K., Bigner, D. D., Van Meir, E. G., Prados, M., Sloan, A., Black, K. L., Eschbacher, J., Finocchiaro, G., Friedman, W., Andrews, D. W., Guha, A., Iacocca, M., O'Neill, B. P., Foltz, G., Myers, J., Weisenberger, D. J., Penny, R., Kucherlapati, R., Perou, C. M., Hayes, D. N., Gibbs, R., Marra, M., Mills, G. B., Lander, E., Spellman, P., Wilson, R., Sander, C., Weinstein, J., Meyerson, M., Gabriel, S., Laird, P. W., Haussler, D., Getz, G. & Chin, L. (2013) The somatic genomic landscape of glioblastoma, Cell. 155, 462-77.

36. Versteege, I., Sevenet, N., Lange, J., Rousseau-Merck, M. F., Ambros, P., Handgretinger, R., Aurias, A. & Delattre, O. (1998) Truncating mutations of hSNF5/INI1 in aggressive paediatric cancer, Nature. 394, 203-6.

37. Margol, A. S. & Judkins, A. R. (2014) Pathology and diagnosis of SMARCB1-deficient tumors, Cancer genetics.

38. Tomlinson, G. E., Breslow, N. E., Dome, J., Guthrie, K. A., Norkool, P., Li, S., Thomas, P. R., Perlman, E., Beckwith, J. B., D'Angio, G. J. & Green, D. M. (2005) Rhabdoid tumor of the kidney in the National Wilms' Tumor Study: age at diagnosis as a prognostic factor, Journal of clinical oncology : official journal of the American Society of Clinical Oncology. 23, 7641-5.

39. Carette, J. E., Raaben, M., Wong, A. C., Herbert, A. S., Obernosterer, G., Mulherkar, N., Kuehne, A. I., Kranzusch, P. J., Griffin, A. M., Ruthel, G., Dal Cin, P., Dye, J. M., Whelan, S. P., Chandran, K. & Brummelkamp, T. R. (2011) Ebola virus entry requires the cholesterol transporter Niemann-Pick C1, Nature. 477, 340-3.

40. Johnson, J. P., Demmer-Dieckmann, M., Meo, T., Hadam, M. R. & Riethmuller, G. (1981) Surface antigens of human melanoma cells defined by monoclonal antibodies. I. Biochemical characterization of two antigens found on cell lines and fresh tumors of diverse tissue origin, European journal of immunology. 11, 825-31.

41. Hsu, P. D., Scott, D. A., Weinstein, J. A., Ran, F. A., Konermann, S., Agarwala, V., Li, Y., Fine, E. J., Wu, X., Shalem, O., Cradick, T. J., Marraffini, L. A., Bao, G. & Zhang, F. (2013) DNA targeting specificity of RNA-guided Cas9 nucleases, Nature biotechnology. 31, 827-32.

42. Wang, H., Yang, H., Shivalila, C. S., Dawlaty, M. M., Cheng, A. W., Zhang, F. & Jaenisch, R. (2013) One-step generation of mice carrying mutations in multiple genes by CRISPR/Cas-mediated genome engineering, Cell. 153, 910-8.

43. Auer, T. O., Duroure, K., De Cian, A., Concordet, J. P. & Del Bene, F. (2014) Highly efficient CRISPR/Cas9-mediated knock-in in zebrafish by homology-independent DNA repair, Genome research. 24, 142-53.

44. Neijenhuis, S., Verwijs-Janssen, M., Kasten-Pisula, U., Rumping, G., Borgmann, K., Dikomey, E., Begg, A. C. & Vens, C. (2009) Mechanism of cell killing after ionizing radiation by a dominant negative DNA polymerase beta, DNA repair. 8, 336-46.

45. Paul, P., van den Hoorn, T., Jongsma, M. L., Bakker, M. J., Hengeveld, R., Janssen, L., Cresswell, P., Egan, D. A., van Ham, M., Ten Brinke, A., Ovaa, H., Beijersbergen, R. L., Kuijl, C. & Neefjes, J. (2011) A Genome-wide multidimensional RNAi screen reveals pathways controlling MHC class II antigen presentation, Cell. 145, 268-83.

46. de Ronde, J. J., Lips, E. H., Mulder, L., Vincent, A. D., Wesseling, J., Nieuwland, M., Kerkhoven, R., Vrancken Peeters, M. J., Sonke, G. S., Rodenhuis, S. & Wessels, L. F. (2013) SERPINA6, BEX1, AGTR1, SLC26A3, and LAPTM4B are markers of resistance to neoadjuvant chemotherapy in HER2-negative breast cancer, Breast cancer research and treatment. 137, 213-23.

47. Trapnell, C., Pachter, L. & Salzberg, S. L. (2009) TopHat: discovering splice junctions with RNA-Seq, Bioinformatics (Oxford, England). 25, 1105-11.

48. Anders, S., Pyl, P. T. & Huber, W. (2014) HTSeq-a Python framework to work with high-throughput sequencing data, Bioinformatics (Oxford, England).

49. Love, M. I., Huber, W. & Anders, S. (2014) Moderated estimation of fold change and dispersion for RNA-Seq data with DESeq2.
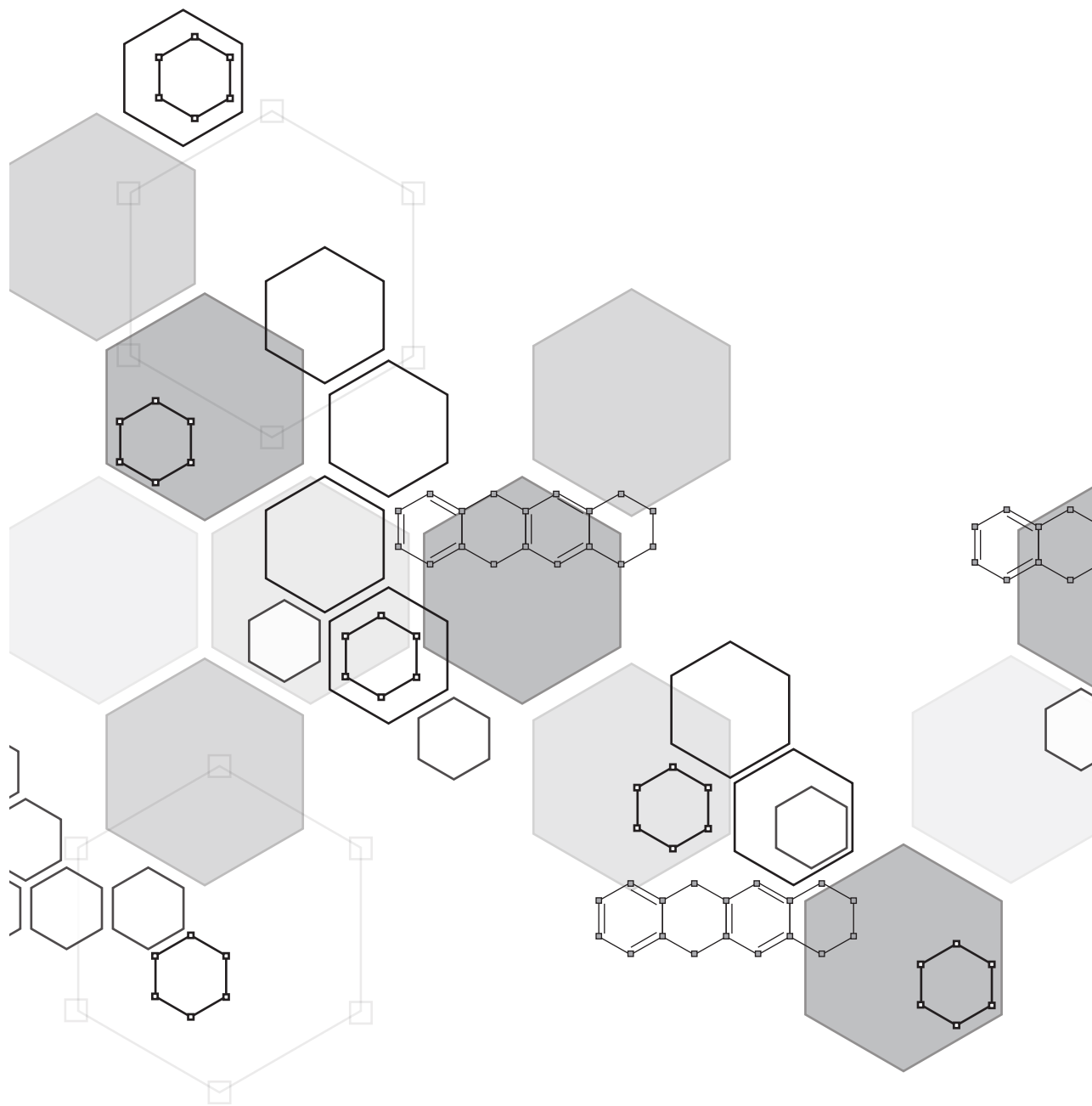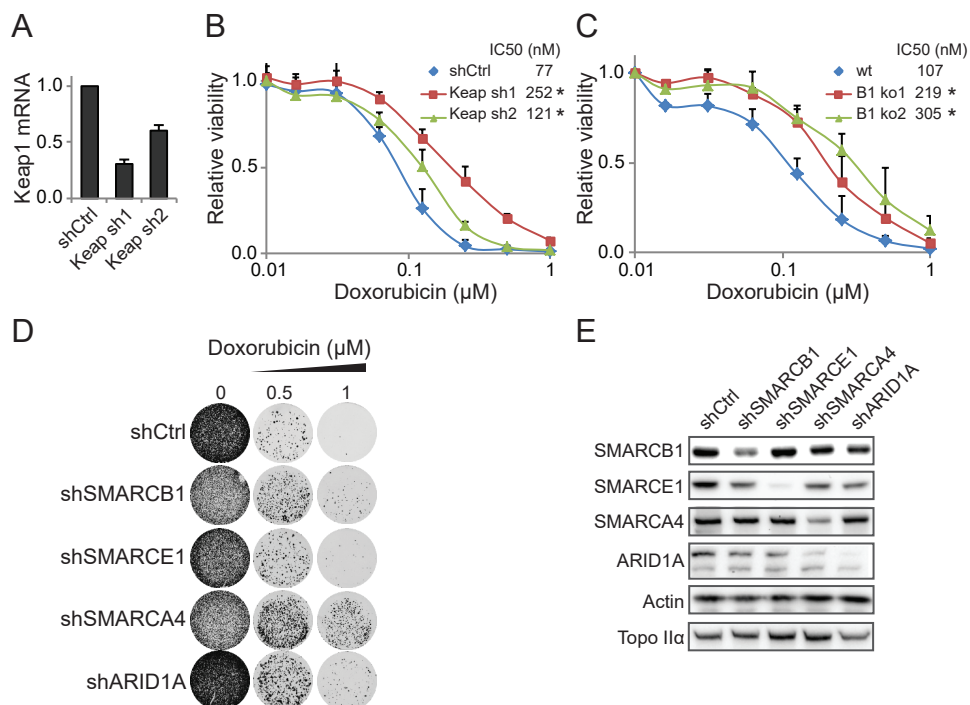
SUPPLEMENTAL INFORMATION

2

Figure S1. Keap1, SMARCB1, SMARCA4 and ARID1A regulate resistance to doxorubicin. *(A) Silencing of Keap1 by shRNAs was measured by qPCR. Keap1 mRNA signal was normalized to GAPDH and shCtrl was set at 1. Shown is the mean ± SD of biological triplicates. (B) Short term growth assay of Keap1-silenced cells incubated with Doxo for 2h at the indicated concentration. Cell viability was analyzed 72 hours after drug removal and extensive washing. Data shown are mean ± SD of biological triplicate experiments. (C) Short-term growth assay as in (B) for wild-type and SmarcB1-depleted cells. Data shown are mean ± SD of biological triplicate experiments. (D) HAP1 cells stably expressing shCtrl or shRNAs targeting SMARCB1, SMARCA4 or ARID1a were treated with Doxo for 2h at the indicated concentrations. Doxo was removed and cells were left to grow out. 9 days later, cells were fixed, stained and imaged. (E) Western blot analysis showing silencing of the respective SWI/SNF complex subunits. Actin is shown as the loading control.*
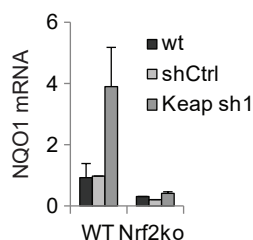

Figure S2. Keap1 controls expression of NQO1 through Nrf2. *mRNA expression analysis of Nrf2 target gene NQO1 using qPCR in cells either or not expressing Nrf2. Expression of NQO1 was calculated relative to GAPDH and data were normalized to WT shCtrl. Results are mean ± SD of biological triplicate experiments.*
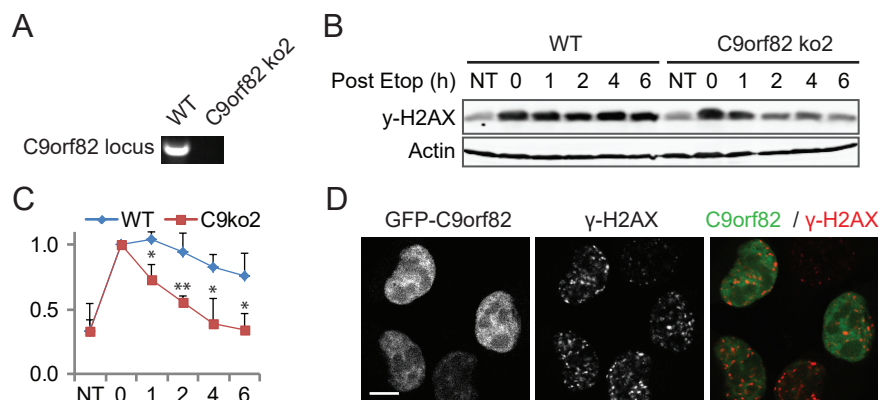
Figure S3. C9orf82 regulates DNA double strand break repair. *(A) DNA gel showing loss of C9orf82 by targeting its locus with a second CRISPR guide RNA. (B) Cells with C9orf82 inactivated were treated with 1µM Etop for 1hr, washed and lysed at the indicated time points post drug removal. Lysates were analyzed by SDS-PAGE and Western blotting analysis for γ-H2AX (upper panel) and actin as the loading control (lower panel). (C) quantification of the γ-H2AX signals from (B), normalized to actin. t=0 was set at 1. Quantification was done from three independent experiments. For all time-points, shown are mean ± SD. (D) MelJuSo cells expressing GFP-C9orf82 were treated for 1 hr with 1µM Etop. Cells were fixed and stained for γ-H2AX before analyses by confocal laser scanning microscope. Bar: 10µm. NT are non-treated cells.*
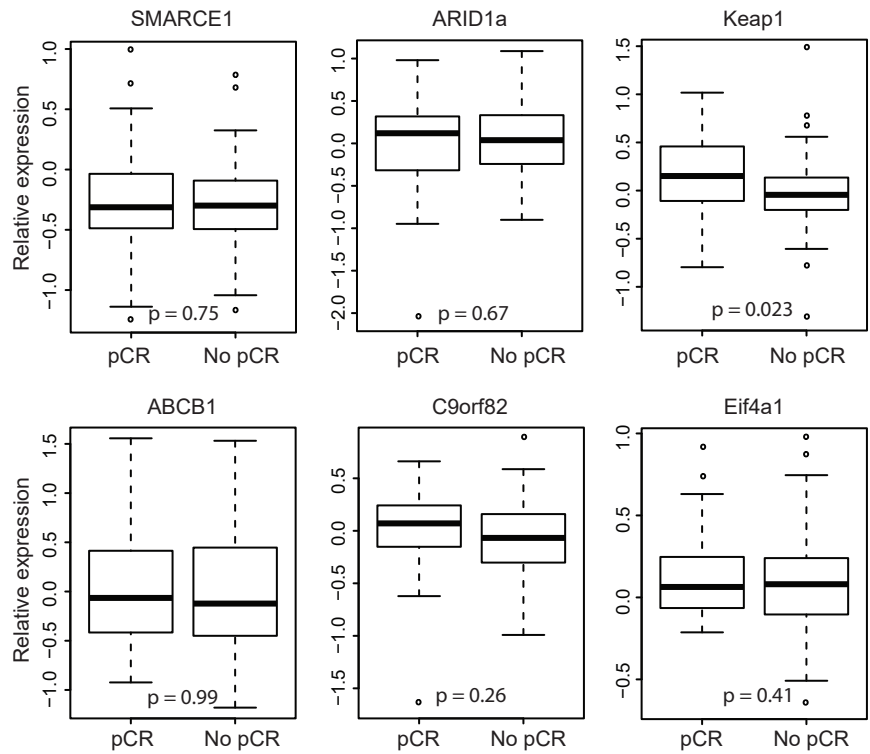
Figure S4. Expression of some SWI/SNF complex subunits correlates to clinical outcome. *Box plot of normalized expression of the indicated genes in 113 triple-negative breast cancer patients that showed pathological complete response (pCR, 46 patients) or not (no pCR, 67 patients) to the treatment with a Doxo containing regimen. p-values were calculated using a Student's T-test.*

Table S1. Overview of all screening hits. *Table can be found online: https://cancerres.aacr-journals.org/content/75/19/4176*

2